

Cold Pools in the Columbia Basin

C. D. WHITEMAN, S. ZHONG, W. J. SHAW, J. M. HUBBE, AND X. BIAN

Pacific Northwest National Laboratory, Richland, Washington

J. MITTELSTADT

NOAA/NWS Forecast Office, Pendleton, Oregon

(Manuscript received 15 June 2000, in final form 15 February 2001)

ABSTRACT

Persistent midwinter cold air pools produce multiday periods of cold, dreary weather in basins and valleys. Persistent stable stratification leads to the buildup of pollutants and moisture in the pool. Because the pool sometimes has temperatures below freezing while the air above is warmer, freezing precipitation often occurs, with consequent effects on transportation and safety. Forecasting the buildup and breakdown of these cold pools is difficult because the interacting physical mechanisms leading to their formation, maintenance, and destruction have received little study.

In this paper, persistent wintertime cold pools in the Columbia River basin of eastern Washington are studied. First a succinct meteorological definition of a cold pool is provided and then a 10-yr database is used to develop a cold pool climatology. This is followed by a detailed examination of two cold pool episodes that were accompanied by fog and stratus using remote and in situ temperature and wind sounding data. The two episodes illustrate many of the physical mechanisms that affect cold pool evolution. In one case, the cold pool was formed by warm air advection above the basin and was destroyed by downslope winds that descended into the southern edge of the basin and progressively displaced the cold air in the basin. In the second case, the cold pool began with a basin temperature inversion on a clear night and strengthened when warm air was advected above the basin by a westerly flow that descended from the Cascade Mountains. The cold pool was nearly destroyed one afternoon by cold air advection aloft and by the growth of a convective boundary layer (CBL) following the partial breakup of the basin stratus. The cold pool restrengthened, however, with nighttime cooling and was destroyed the next afternoon by a growing CBL.

1. Introduction

A cold pool is a topographically confined, stagnant layer of air that is colder than the air above. Cold pools can be characterized as *diurnal*, forming during the evening or night and decaying following sunrise the next day, or as *persistent*, lasting longer than a normal nighttime temperature inversion. Diurnal cold pools are surface-based stable layers that are a common fair weather feature of valley and basin meteorology. Their depth and strength depend largely on the characteristics of the surrounding terrain and the synoptic weather situation. Persistent cold pools are temperature inversions that occur primarily in winter when the daily cycle of sensible heating and convection are insufficient, either because of cloudiness or seasonal reductions of sensible heat flux, to destroy the stable layer on a daily basis.

Since a cold pool is stably stratified and the winds within the pool are weak, air pollution or moisture emit-

ted into the cold pool undergo very limited dispersion, sometimes leading to severe air pollution episodes. When stratiform cloudiness develops within cold pools, prolonged periods of relatively cold, dreary weather can occur. Liquid precipitation falling into a subfreezing cold pool produces freezing rain or drizzle, with attendant disruption of transportation and other human activities. Cold pools can also lead to delays in the melting of snow and the breakup of ice on rivers. The breakup of persistent cold pools is particularly difficult to forecast and is considered one of the most challenging forecast problems in complex terrain areas of the United States (Smith et al. 1997).

In this paper, we investigate the evolution of two persistent cold pools that formed in the Columbia River basin of eastern Washington in December of 1998 and January of 1999 using analyses of meteorological data from both operational and research instrumentation. These episodes were the two major cold pool events of the winter of 1998/99 and they illustrate different processes of formation and destruction of cold pools in this basin. A companion paper (Zhong et al. 2001) utilizes a mesoscale numerical model to investigate the January

Corresponding author address: C. D. Whiteman, K9-30, Battelle Northwest Laboratories, P.O. Box 999, Richland, WA 99352.
E-mail: Dave.Whiteman@pnl.gov

episode further. In section 2, we provide a brief summary of previous research on persistent wintertime cold pools. Section 3 describes the research sites and measurements, section 4 the climatology of cold pools in the Columbia basin, and section 5 two cold pool episodes in the Columbia basin. This is followed, in section 6, by a further discussion of several aspects of the analyses. Conclusions are presented in section 7.

2. Previous research

While the evolution of diurnal cold pools has received a great deal of study (see the review by Whiteman 1990), the evolution of persistent cold pools has received little research attention despite their frequent occurrence in valley and basin settings in many parts of the world. The serious logistical problems encountered in running wintertime field studies, the difficulty and expense of making frequent vertical soundings through the cold pool with the requisite resolution of temperature and wind structure near the top of the pool, and limitations on modeling imposed by the need for high vertical resolution of the shallow slope flows and processes taking place in the upper cold pool have all contributed to this situation. It is only recently that suitable remote sensing instruments have become available and computer power and model formulations have been improved so that the processes affecting persistent cold pools can be studied in depth.

Air pollution problems in cold pools that form in the basins of Slovenia and Croatia have been widely recognized and studied (Petkovšek 1978, 1980, 1992; Vrhovec 1991; Vrhovec and Hrabar 1996), although no data are yet available on the evolution of vertical wind and temperature structure during the cold pool episodes. In wintertime, these basins are often capped by low clouds that decrease insolation and cause cold air pools to last for many days (Petkovšek 1974). Vertical soundings of diurnal cold pools that form in Austria's Gstettner-Alm sinkhole were made in Europe as early as 1953 with the aid of a resistance thermometer carried aloft by a tethered balloon (Sauberer and Dirnhirn 1954). The cold pools that form there lead to wintertime temperature minima that can reach -50°C . These extreme temperatures are reached overnight in the small basin when the ground is covered by snow and the sky is clear. The extreme cooling is produced by longwave radiation loss following an early drainage of cold air into the basin from the surrounding sidewalls on the previous afternoon.

In the United States, persistent midwinter cold pools are known to form over the Colorado Plateau (Whiteman et al. 1999a) under clear or partly cloudy conditions following arctic air intrusions or simply following clear nights when cold air drains into the basin from surrounding mountain areas. Convective boundary layers warm the base of the cold air pool during daytime but the wintertime heating is often insufficient to break

through the deep pool. The pool strengthens or weakens as weather systems pass through the Southwest with their associated warm and cold air advection above the pool and as daytime convective boundary layers and nighttime stable boundary layers modify the base of the pool. Strong temperature jumps can be produced above cold air pools when warm air advection occurs aloft. These jumps, particularly evident above narrow confined topography, have been reported above the Grand Canyon (Whiteman et al. 1999b).

Persistent stagnation episodes in the Great Basin of the western United States are related to cold pool formation and have been studied climatologically using rawinsonde and other data (Wolyn and McKee 1989; Savoie and McKee 1995). Some of the cold pool or stagnation events in this large intermountain area are produced by flow blocking upstream of the Rocky Mountains (Mayr and McKee 1995). The flow can become unblocked rather abruptly by passing short-wave troughs.

The Columbia basin is intermediate in scale between the small Slovenian, Croatian, and Austrian basins and the larger Colorado Plateau and Intermountain basins. The present paper includes a brief discussion of the differences between the cold pools that form in the Columbia basin and the Colorado Plateau.

3. Sites and measurements

The Columbia basin (Fig. 1) of eastern Washington and Oregon is located between the Cascade and Rocky Mountains. The basin is in the form of a saucer tilted downward to the southwest with its lowest point in the Pasco, Washington, subbasin. The Columbia River leaves the Pasco subbasin by flowing southeastward and then turning abruptly westward through a narrow defile (the Wallula Gap) into the upper end of the Columbia Gorge, located on the boundary between the states of Washington and Oregon. The Pasco subbasin is the scene of persistent cold pool episodes each winter. In these episodes, cold air remains trapped in the basin, usually accompanied by fog and stratus clouds. The prediction of the buildup and breakup of the Columbia basin cold air pool is one of the most difficult forecast problems in the region—a problem exacerbated by the lack of routine upper air soundings in the basin.

In the winter of 1998/99, meteorological research instruments were installed and operated in the Pasco subbasin to provide temperature and wind profiles to supplement existing networks of routinely operated meteorological stations and to provide, for the first time, definitive observations of the Columbia basin cold pool. The instrumentation is described below; instrument sites are shown in Fig. 2.

First, a five-beam, 915-MHz radar wind profiler (RWP) with a radio acoustic sounding system (RASS) was operated at the Hanford Meteorological Station [HMS, 223 m above mean sea level (MSL)] in the Pasco

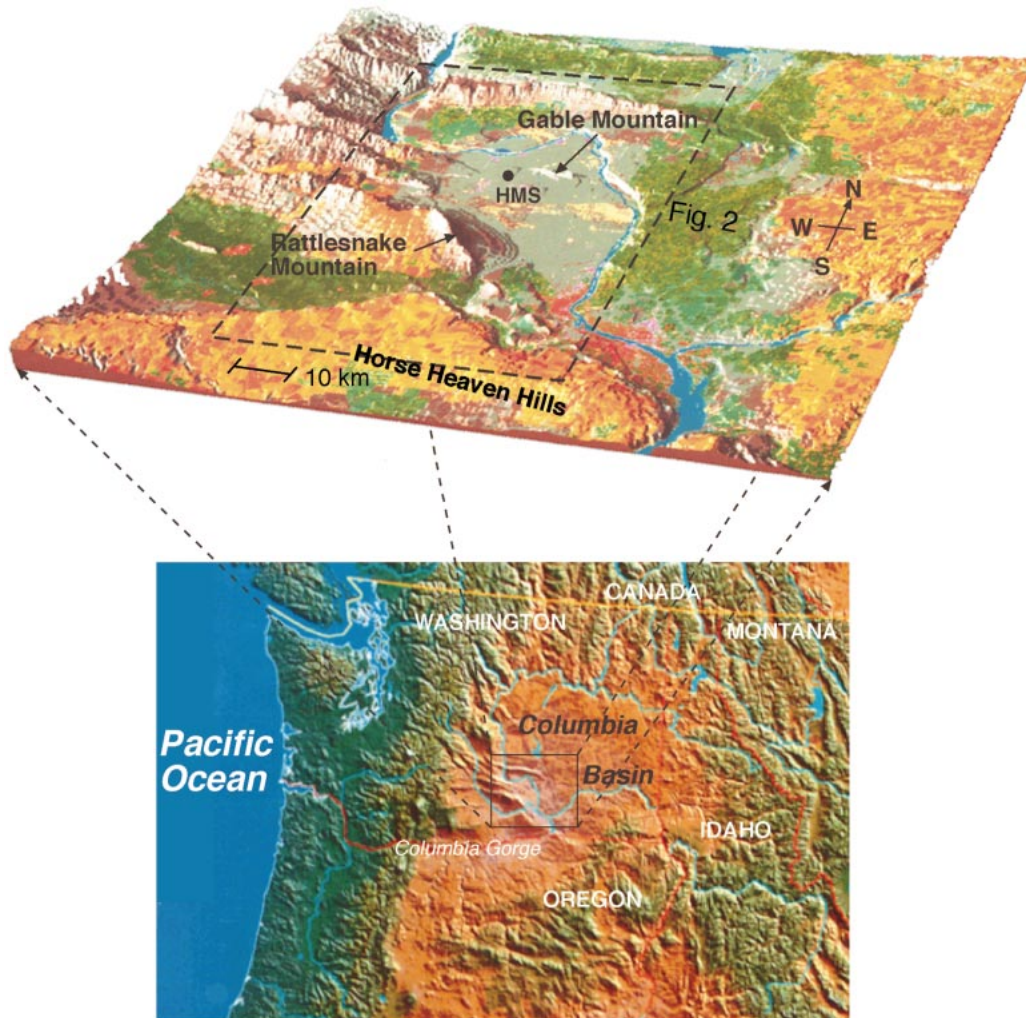


FIG. 1. Plan map of the Pacific Northwest, showing the Columbia basin on the east side of the Cascade Mountains. The upper part of the figure presents a three-dimensional view of the Pasco subbasin showing the locations of Rattlesnake and Gable Mountains and the Hanford Meteorological Station (HMS). The dashed line shows the domain of Fig. 2.

subbasin. The RWP reported vertical profiles of mean horizontal wind every half hour as averaged over 100-m elevation intervals and over 20-min averaging periods from 10 to 30 min and from 40 to 60 min after each hour. The RASS reported vertical profiles of virtual temperature every half hour, as averaged over 100-m range gates and over 10-min averaging periods from 0 to 10 min and from 30 to 40 min after each hour. The accuracy of radar profiler winds and RASS virtual temperatures are reported to be $\pm 1 \text{ m s}^{-1}$ and $\pm 1^\circ\text{C}$ (Furger et al. 1995).

Second, two lines of Hobo[®] temperature dataloggers (Onset Computer Corp., Bourne, MA) were placed on the steep, northeast-facing slope of Rattlesnake Mountain (1074 m MSL) and on the east-facing slope of Gable Mountain (332 m MSL). These slopes are uniform surfaces containing no major tributaries, with no forested

areas, and with a surface cover of natural grasses and shrubs. Rattlesnake Mountain is located at the end of a long ridge called the Rattlesnake Hills that extends southeastward into the Columbia basin from the Cascade Mountains (Fig. 1). Gable Mountain, a short, east-west ridge, is located in the interior of the Pasco subbasin north of Rattlesnake Mountain near the Columbia River (Fig. 1). The 11 dataloggers on the Rattlesnake Mountain and the 3 dataloggers on the Gable Mountain lines (see Fig. 2) were generally spaced at 100-m elevation intervals. The lowest datalogger on each mountain slope was located close to the mountain base in a river valley (Yakima River for Rattlesnake Mountain and Columbia River for Gable Mountain). The dataloggers were exposed on steel fence posts with their thermistors 1 m above ground level inside 6- or 12-plate radiation shields. The loggers sampled and stored tem-

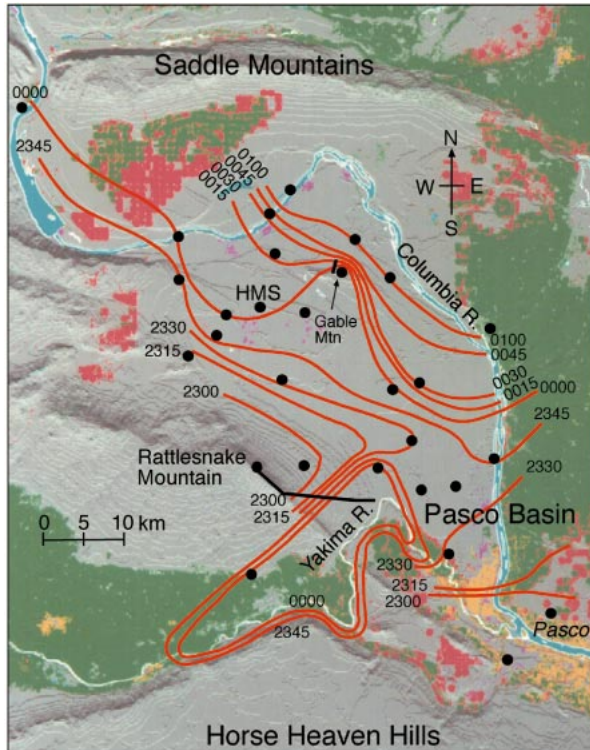


FIG. 2. Plan view of the Pasco subbasin domain indicated in Fig. 1. Shown are the major topographic features and the instrument sites. The filled dots are the HMMN stations, the dark lines on Rattlesnake and Gable Mountains indicate the mountainside lines of temperature dataloggers, and HMS indicates where the radar wind profiler, RASS, 122-m instrumented tower, and manned weather station were located. The lines labeled with times (LST) indicate frontal positions at 15-min intervals on 25–26 December 1998 as a pseudo-warm front passed across HMMN, destroying the Columbia Basin cold pool.

perature readings every 5 min. Laboratory investigations of the accuracy ($\pm 0.4^{\circ}\text{C}$), resolution (0.01°C), and time constants (122 s) of the temperature dataloggers have been reported by Whiteman et al. (2000). When used in the field, the thermistor sensors are subject to additional inaccuracies that depend on their exposure to solar and terrestrial radiation and wind speed. The thermistor sensors were exposed in R. M. Young Model 41301-5 nonaspirated radiation shields. These and similar shields have been extensively tested (Gill 1983, or the references in Whiteman et al. 2000). The root-mean-square temperature excess in this shield for solar radiation of 1080 W m^{-2} is expected to be 0.4°C in 3 m s^{-1} winds, 0.7°C in 2 m s^{-1} winds, and 1.5°C in 1 m s^{-1} winds. In our winter experiments the solar radiation loading of the shields was low, but winds within the pool were also weak.

Third, data were collected from a preexisting operational network (the Hanford Meteorological Monitoring Network, HMMN) of meteorological sensors located on 30 10-m towers that were distributed within a 55-km radius of HMS (Fig. 2). All of the network stations reported 15-min averages of temperature, wind, pres-

sure, and precipitation data. Four of these stations also reported relative humidity data. Temperature and relative humidity data are from a height of 2 m, while wind data are from 10 m.

Fourth, 15-min-average temperature and wind data were obtained from a 122-m tower at HMS. Temperature measurements were made at the 0.9-, 9.1-, 15.2-, 30.5-, 61.0-, 76.2-, 91.4-, and 121.9-m levels. Wind measurements were made at the 9.1-, 15.2-, 61.0-, and 121.9-m levels. The foot of this tower is at 223 m MSL. Calibrations are maintained on the tower so that temperature data are expected to be accurate to 0.2°C ; humidity accuracy is about 5%. This tower was within 400 m of the radar wind profiler—RASS, providing data below the first range gates of these two remote sensing instruments.

Finally, hourly surface observations (including cloud observations) were made at HMS, which was staffed 24 h per day on weekdays and 8 h per day on weekends.

4. Climatology of the Columbia basin cold pool

Because no rawinsonde stations are located in the lower Columbia basin (the nearest is at Spokane, WA, 205 km NE of Pasco at an elevation of 728 m, 505 m higher than HMS), we used data from surface meteorological stations to develop a climatology of cold pools. This was done using hourly data from two surface stations: one on the summit of Rattlesnake Mountain (generally above the cold pool) and one from HMS (near the base of the cold pool). We examined data for the months October through March for the period from 1 January 1989 through 31 March 1999. A persistent cold pool was considered to be present in the lower Columbia basin if 1) a temperature inversion was present between the two sites, 2) wind speeds at HMS were below 3.1 m s^{-1} (7 mph), and 3) these conditions persisted for 18 h or more. This last criterion effectively removed *diurnal* cold pools from the climatology. The results were as follows: 120 persistent cold pool events occurred over the 1989–99 period, with durations between 18 and 103 h (median duration 28.5 h). The mean number of persistent cold pools per month and mean duration are shown in Fig. 3. From the figure, cold pools are clearly a midwinter phenomenon, with the peak frequency of occurrence in December and January. Many cold pool episodes persist for less than 24 h but, in many instances, two or more cold pools form successively, being separated by short pauses when the cold pool criteria are not met either because of a temporary decrease in atmospheric stability or an increase in surface winds. In these cases, an observer in the cold pool might consider the cold pool to have a longer duration than indicated by the climatology. The cold pool episodes to be discussed in this paper occurred during a winter with a relatively small number of cold pools (one in October, five in December, and three in January) and, except for January, below-average durations.

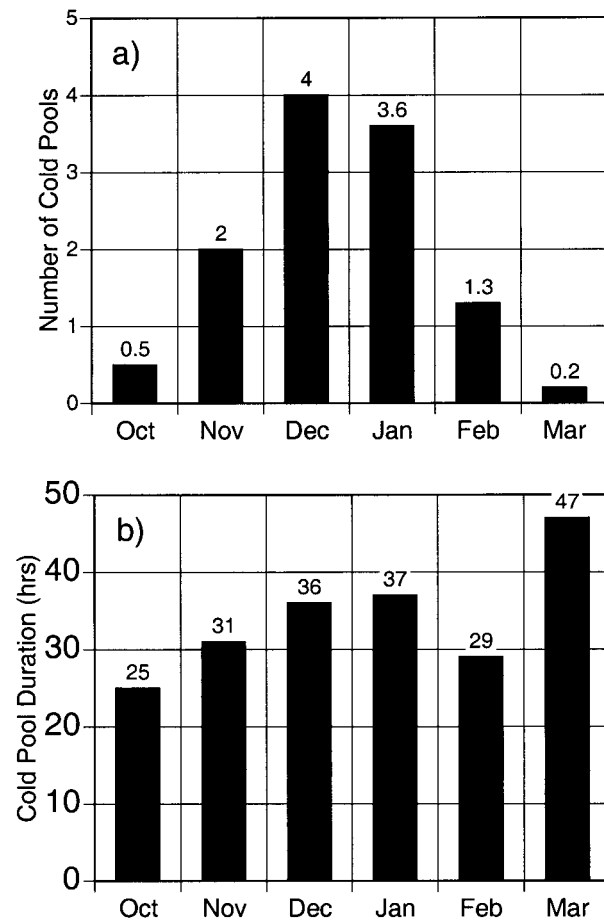


FIG. 3. (a) Mean monthly number and (b) duration of cold pools in the lower Columbia basin, based on data from Oct through Mar for the period from 1 Jan 1989 through 31 Mar 1999. Cold pools occur when the Rattlesnake Mountain temperature equals or exceeds that at HMS, HMS winds are less than or equal to 3.1 m s^{-1} (7 mph), and these conditions prevail for 18 h or more.

The temperature difference and wind speed criteria used to define a cold pool are somewhat arbitrary, given the nonideal locations (i.e., elevations) of the HMS and Rattlesnake Mountain stations. The mountain site (1074 m MSL) may be well above the basin temperature inversion top when inversions are shallow, and the HMS site (223 m MSL), located on a small plateau, often has

higher temperatures and wind speeds than would be experienced under inversion conditions at lower elevations near the Columbia River. For this reason, the number of cold pool cases and their mean duration are presented in Table 1 for alternate choices of temperature difference and wind speed criteria. The number of cases and the mean duration are affected only slightly by changing the wind speed criteria, but are rather sensitive to the temperature difference (atmospheric stability) criteria.

5. Two cold pool episodes

a. 24–26 December 1998

An arctic cold front moved through the Columbia basin on 19 December 1998 ushering in a cold northerly flow that continued through 23 December and filled the Columbia basin with cold air. Minimum temperatures in the Columbia basin fell from 0° to -5°C on 18 December to -15° to -20°C on 23 December. A weak upper-level short wave turned the flow aloft from northerly to westerly late on 23 December, and on 24 December a strong Pacific low pressure system approached the Pacific Northwest coast. An associated warm front moved northward along the Oregon coast the afternoon of 24 December with warm air advected in advance of this front over the Columbia basin. A variety of precipitation types were observed in the basin during this warm advection period including rain, freezing rain, and snow.

The destruction of the cold pool was accomplished as a pseudo-warm front traveled northeastward across the Pasco subbasin at a speed of approximately 10 km h^{-1} between 2300 LST 25 December and about 0200 LST 26 December. Isochrones of the frontal positions at 15-min intervals are shown in Fig. 2. Fifteen-minute-average surface winds behind the retreating cold air were generally west-southwesterly at 10 or 12 m s^{-1} . Before the frontal passage, temperatures over the subbasin were around -7°C , with temperatures on Rattlesnake Mountain near 0°C . Following the frontal passage, temperatures warmed to 7°C and, with the weakly stable atmosphere that prevailed after the frontal passage, Rattlesnake Mountain had cooler temperatures (again, about 0°C) than the stations on the basin floor. The

TABLE 1. Cold pool number and mean duration in h (table cell entries separated by a comma) in the period from 1 Jan 1989 through 31 Mar 1999 for various temperature difference and wind speed criteria. $T_{\text{RAT}} - T_{\text{HMS}}$ is the temperature difference criterion between Rattlesnake Mountain and HMS; ws is the wind speed criterion at HMS. The criteria chosen for our reported climatological results are set in boldface.

$T_{\text{RAT}} - T_{\text{HMS}}$ ($^\circ\text{C}$)	$ws \leq 2.2$ (m s^{-1})	$ws \leq 3.1$ (m s^{-1})	$ws \leq 4.0$ (m s^{-1})	$ws \leq 4.9$ (m s^{-1})	$ws \leq 5.8$ (m s^{-1})
≥ -3.33	215, 30.1	290, 34.8	324, 36.9	333, 37.6	338, 38.1
≥ -2.22	167, 30.4	208, 35.7	230, 37.4	236, 38.0	241, 38.0
≥ -1.11	129, 30.7	157, 35.2	169, 37.3	175, 37.5	176, 37.7
$\geq \mathbf{0.00}$	93, 31.3	120, 34.6	125, 37.1	128, 37.4	128, 37.8
≥ 1.11	60, 30.5	81, 31.7	85, 34.4	88, 34.4	88, 34.8
≥ 2.22	40, 28.4	58, 28.1	58, 31.1	59, 31.4	60, 31.6
≥ 3.33	26, 26.6	37, 26.3	40, 27.7	40, 27.9	40, 28.1

frontal positions, analyzed from wind speed and direction shifts and temperature gradients, remained parallel to the mountain ridgeline on the southwest edge of the basin as it traveled across the basin (Fig. 2), suggesting that the flow over Rattlesnake Mountain and its ridgeline extension to the SE plays an important role in organizing the frontal passage across the basin floor. Also seen in the frontal analysis was the trapping of cold air at the lowest elevations in the Yakima and Columbia valleys, with the warmer air simply overrunning the shallow cold air remnants. This feature of cold pool destruction has been previously observed by forecasters at HMS (P. J. Perrault 1999, personal communication).

The interesting synoptic environment leading to the destruction of the Pasco subbasin cold pool by the slowly moving pseudo-warm front will be discussed by reference to 850 hPa (Fig. 4) and surface (Fig. 5) charts, as well as to time series of weather observations at HMS and Rattlesnake Mountain (Fig. 6). A high in the southwestern United States continued to support ridging over the Columbia basin at 0400 LST on Christmas morning, but a deep trough was approaching Washington from the west (Fig. 4a). By 1600 LST, a closed low developed over the northern Puget Sound and 850-hPa temperatures over the Pasco subbasin had warmed from -3° to 0°C . The pressure gradient tightened both south and east of the low pressure center, supporting strong southeasterlies over the subbasin and strong westerlies over the Columbia Gorge (Fig. 4b). By 0400 LST on 26 December, the low had moved eastward across the Columbia basin, filling, and forming a short-wave trough in central Montana (Fig. 4c). Cold air advection along with some weak nighttime cooling after the clouds dissipated caused the 850-hPa temperature over the Pasco basin to drop back to -3°C .

Because the basin cold pool was destroyed between the 12-hourly upper air sounding times, sea level pressure analyses at 1900, 2200, and 0100 LST (Fig. 5) are used to gain further insight into the cold pool destruction process. At 1900 LST (Fig. 5a), a surface low that trailed the eastward-moving upper-level disturbance was in the Puget Sound area. A surface low pressure center began to develop in the Columbia basin as the upper-level disturbance crested the Cascades, and strong southerly winds were found in eastern Oregon south of the Pasco subbasin. By 2200 LST (Fig. 5b), the surface low east of the Cascades had deepened and moved farther eastward to the Spokane area as the upper-level disturbance passed. Winds shifted to the west in northern Oregon, bringing warm marine air up the Columbia Gorge while, in the upper gorge, winds strengthened and began to shift to the southwest, carrying air over the Horse Heaven Hills and the Rattlesnake ridge into the low pressure center in the Columbia basin. The destruction of the cold pool in the Pasco basin occurred during the brief time when these winds shifted across the Rattlesnake ridge, producing their strongest cross-ridge component and producing strong downslope winds on the lee or

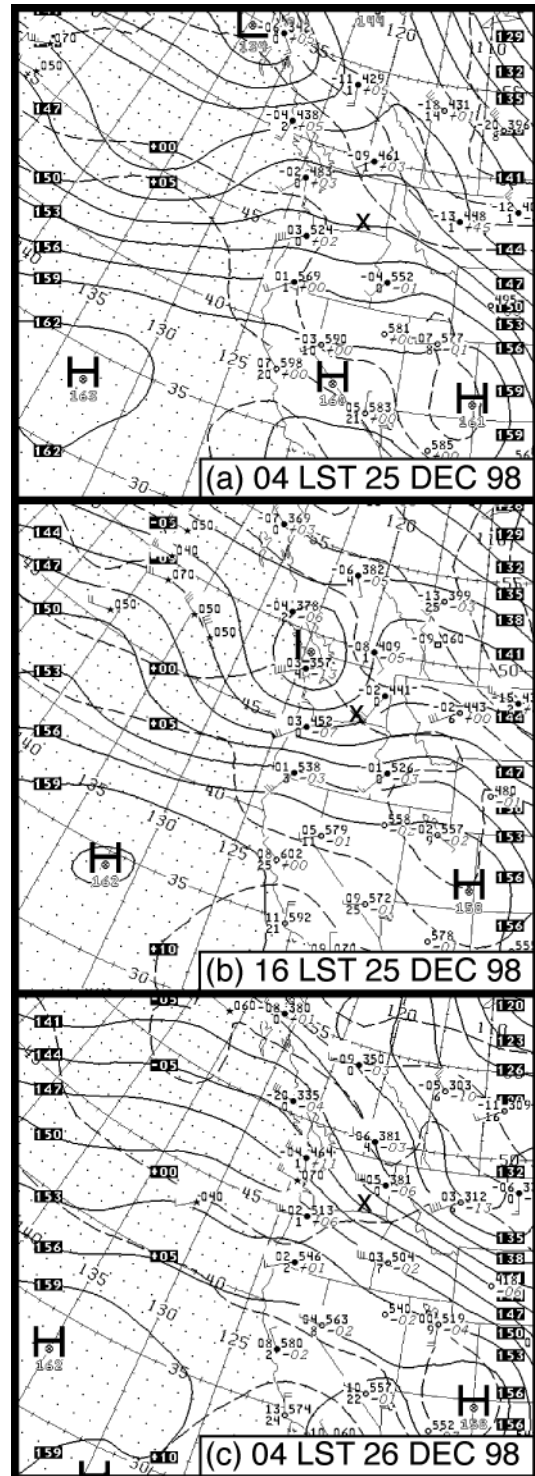


FIG. 4. Sequence of 850-hPa analyses for the Dec 1998 cold pool episode, at (a) 0400 LST 25 Dec, (b) 1600 LST 25 Dec, and (c) 0400 LST 26 Dec. An \times marks the location of HMS on each chart. (From National Climatic Data Center.)

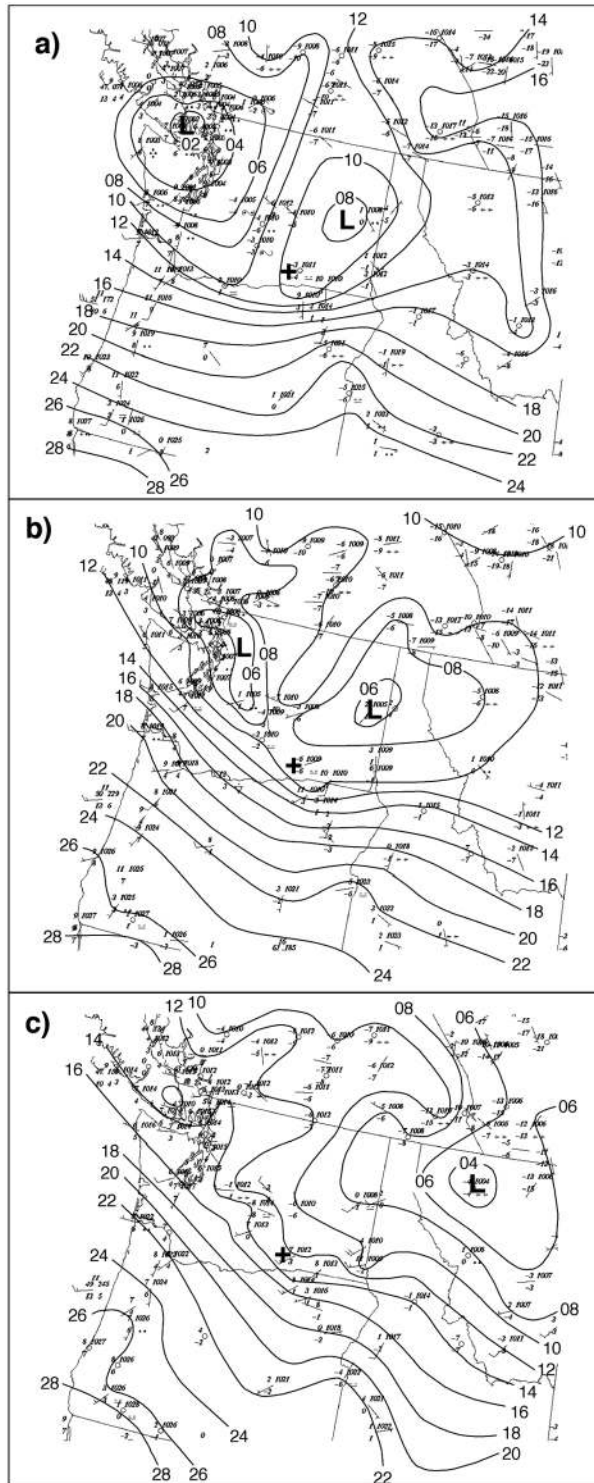


FIG. 5. Sequence of sea level pressure analyses for the Dec 1998 cold pool, at (a) 1900 LST 25 Dec, (b) 2200 LST 25 Dec, and (c) 0100 LST 26 Dec. A + marks the location of HMS. Sea level pressure is contoured at 2-hPa intervals, with the last two digits shown. The station model includes temperature and dewpoint in $^{\circ}\text{C}$ and winds in m s^{-1} , with a single barb indicating 10 and a half barb indicating 5 m s^{-1} .

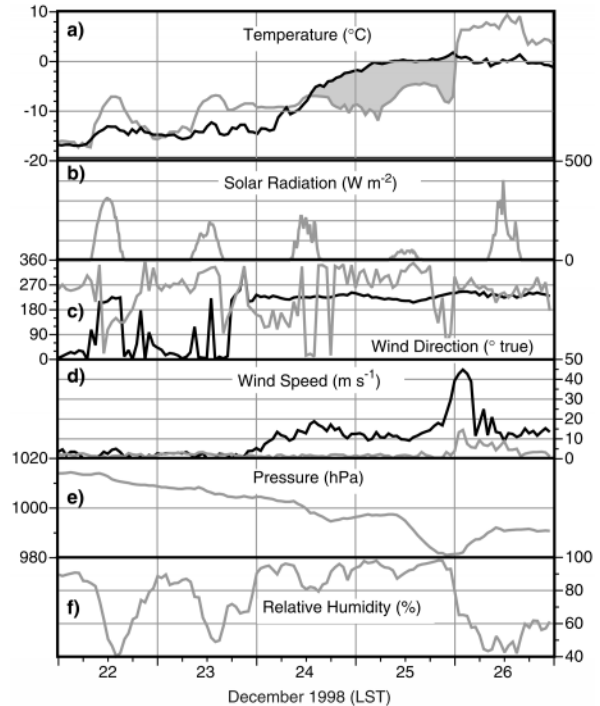


FIG. 6. Time series of meteorological variables at Rattlesnake Mountain (black lines) and HMS (gray lines) for the Dec 1998 cold pool. Shading indicates the cold pool period.

northeast side of the mountain. The cold air in the basin was carried northeastward by the descending winds, with mixing enhanced by shear at the cold pool interface in the pseudo-warm frontal zone. By 0100 LST (Fig. 5c), cold pool destruction was nearly complete in the Pasco subbasin, winds coming over the Rattlesnake ridge were shifting into a more westerly direction and, farther north, stronger west winds were bringing warm marine air through the mountain gaps over the Cascade Mountains and down the lee side of the Cascade Mountains. Cold air at the northern end of the Columbia basin did not mix out until later when these west winds became stronger. Moses Lake, 110 km north of Pasco, did not experience the rapid warming until 0700 LST 26 December.

Figure 6 shows time series of surface temperature, solar radiation, wind direction, wind speed, pressure, and relative humidity at HMS during the entire cold pool episode and, for comparison, temperature, wind direction, and wind speed at the summit of Rattlesnake Mountain. The buildup of the cold pool was produced by a strengthening southwest wind above the basin that began in the late evening of 23 December (Figs. 6c and 6d) and produced warm air advection aloft (Fig. 6a). This warming, when combined with a nearly constant temperature at the floor of the partly cloudy basin, which received little insolation (Fig. 6b), produced a basin temperature inversion and cold pool by noon on 24 December. Winds at the basin floor were below 3.1 m s^{-1}

and from the northwest quadrant during the cold pool episode. Winds aloft were from the southwest, generally at speeds of 10–20 m s⁻¹, except near the end of the cold pool episode when they became very strong, reaching 46 m s⁻¹ on the summit of Rattlesnake Mountain. Freezing rain and ice pellets produced an accumulation of 0.09 in. (2.3 mm) of melted precipitation in the basin between 1000 and 1600 LST on 25 December. Cold pool destruction occurred as the temperature aloft remained steady and the temperature at the basin floor warmed rapidly as the previously mentioned pseudo-warm front progressed across the Pasco subbasin. Pressure decreased through much of the cold pool episode as the trough approached (Fig. 6e), but a rapid pressure rise followed after passage of the short-wave trough. Relative humidity varied from 80% to 96% during the episode (Fig. 6f), but decreased rapidly following cold pool breakup.

The evolution of vertical temperature and wind structure in the Pasco subbasin during the cold pool breakup period is shown in Fig. 7, which includes data from the radar profiler–RASS, the instrumented tower, the surface-based temperature loggers on the mountainsides, and wind observations from Rattlesnake Mountain. At 1800 LST (Fig. 7a), both the RASS and temperature loggers indicated that the cold pool top was at about 700 m MSL. The temperature profile below the top of the cold pool exhibited a near-moist-adiabatic lapse rate indicative of stratiform clouds in the cold pool. By 2100 LST (Fig. 7b), the stability at the top of the cold pool had strengthened and the top had lowered to 450 m MSL over the northeast slope of Rattlesnake Mountain while still maintaining an elevation of 700 m MSL over HMS. While no wind data were available on the slope, the depression of the cold pool top at this time and the slightly stable atmosphere above the cold pool is consistent with a lee wave or hydraulic flow on the northeast side of the mountain as a southwest flow carried stable air directly across the ridge crest. Between 2300 and 0000 LST, the pseudo-warm front produced at the interface between the warm air descending the lee slope and the southwestern edge of the cold pool propagated across the terrain between Rattlesnake Mountain and HMS destroying the remnants of the cold pool on the plateau. The remnants of the cold pool were still present, however, in the low-lying terrain near the Columbia River north of Gable Mountain (open circles in Fig. 7c). The cold pool destruction was complete at HMS by about 0235 LST as static stability decreased above the cold pool, vertical mixing became stronger, and winds shifted to westerly, decreasing the cross-ridge component of the flow. Figure 7d shows the temperature and wind structure at 0525 LST, when the atmosphere was well mixed above the site and strong westerly winds were present through most of the basin atmosphere.

b. 2–7 January 1999

The 500-hPa geopotential height pattern during the 2–7 January cold pool episode was characterized by a

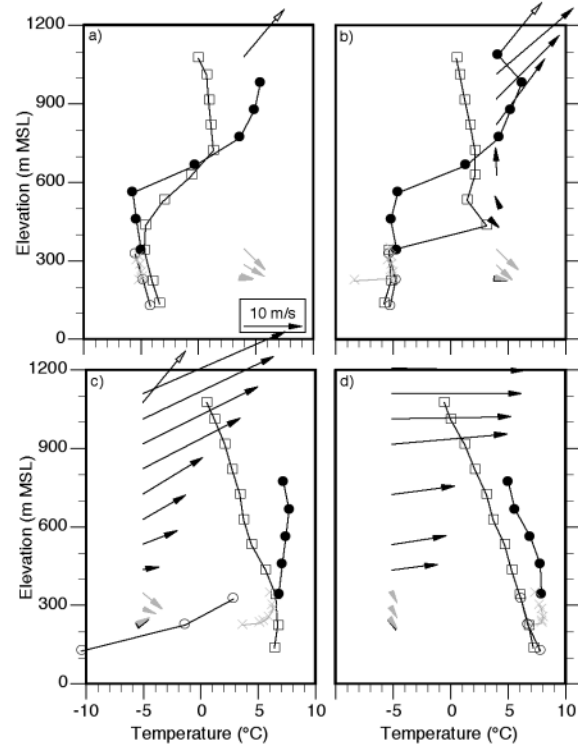


FIG. 7. Evolution of vertical temperature and wind structure as the Columbia basin cold pool is destroyed by a pseudo-warm front passage on 25–26 Dec 1998 at (a) 1800, (b) 2100, (c) 0000, and (d) 0525 LST. The RASS curve (solid circles) is virtual temperature; other curves are temperature (Rattlesnake, square; Gable, circle; tower, \times). The open arrowheads are surface wind vectors on Rattlesnake Mountain, gray vectors are tower winds, solid vectors are RWP winds. Conversion of virtual temperature to actual temperature requires humidity measurements, which were unavailable. The maximum correction, obtained by assuming a relative humidity of 100%, would decrease the RASS curve between 0.3° and 1.4°C, with the largest correction at the warmest temperature.

broad, deep trough over the central and eastern United States with a quasi-stationary ridge over or slightly upstream of the entire west coast of North America. The Pacific Northwest, located east of the ridge axis, had contours that were oriented from northwest to southeast. Northwestern flow prevailed over the Pacific Northwest, with some day-to-day variations due to the passage of minor short-wave troughs. The surface pattern included a high pressure center that drifted from day to day over the Pacific Northwest, with no frontal systems nearby during the period. Figure 8 provides a series of synoptic weather analyses at 24-h intervals to illustrate the evolution of the 850-hPa geopotential height and temperature patterns during the cold pool episode. The 850-hPa pressure level is approximately 400 m above Rattlesnake Mountain and, thus, provides information on warm and cold air advection above the basin cold pool. The warmest temperatures at 850 hPa during the episode were located just off the West Coast under the mean ridge position. At 1600 LST 2 January 1999 at

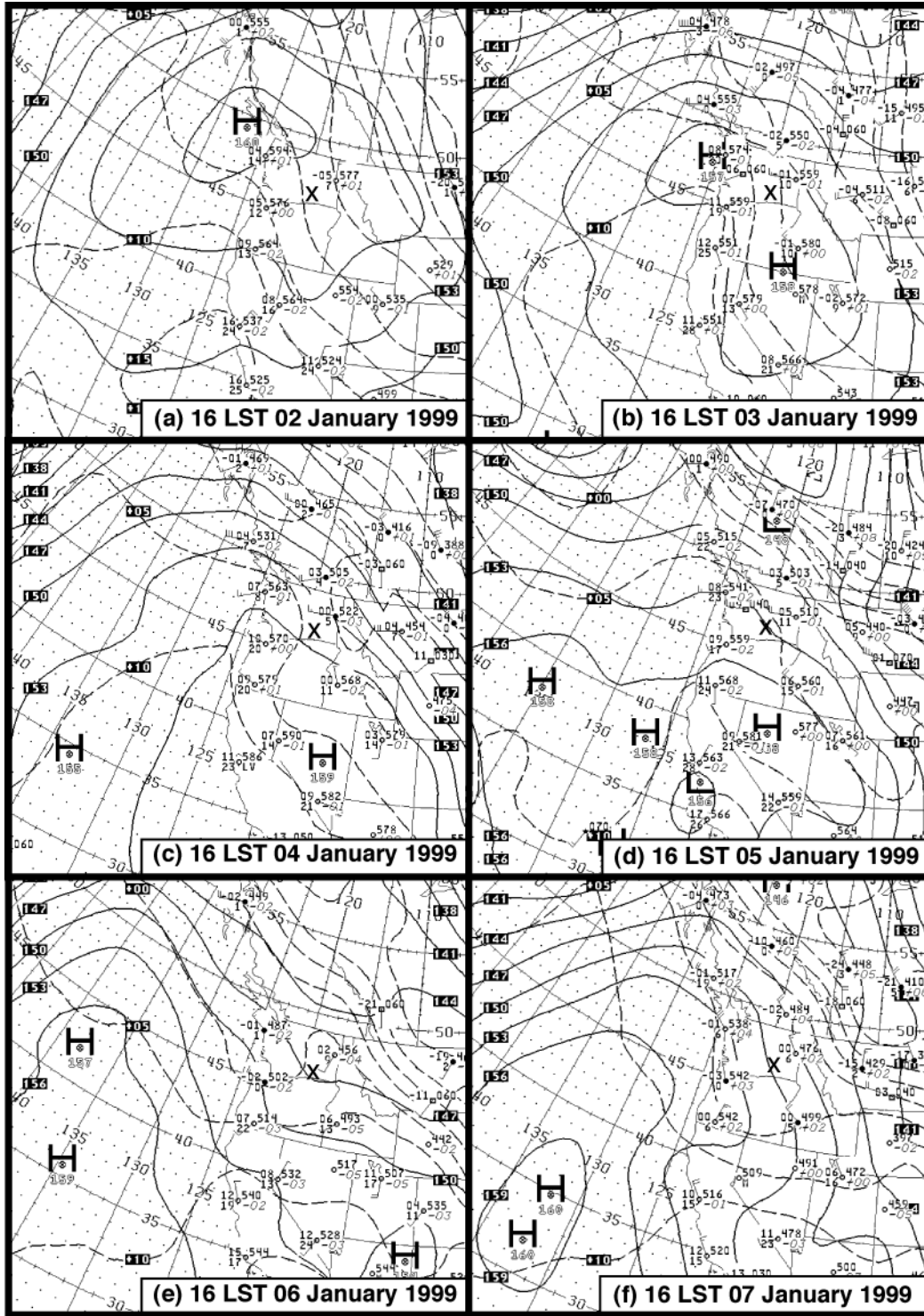


FIG. 8. Series of 850-hPa upper air analyses at 24-h intervals between 1600 LST 2 Jan and 1600 LST 7 Jan 1999. Solid lines are geopotential height contours in dm; dashed lines are temperature contours in °C. An X marks the location of HMS. (From the National Climatic Data Center.)

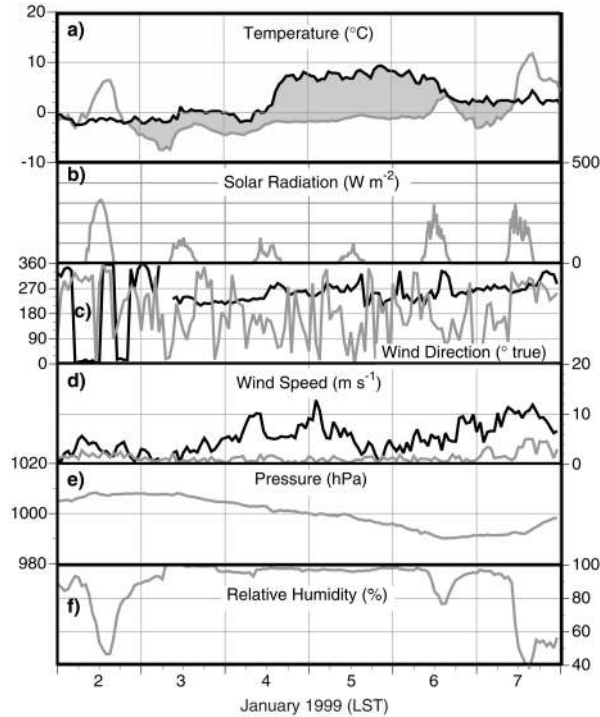


FIG. 9. Time series of meteorological variables at Rattlesnake Mountain (black lines) and HMS (gray lines), 2–7 Jan 1999. Shading indicates the cold pool period.

the beginning of the episode (Fig. 8a) the 850-hPa temperature was about -1°C over the Pasco basin. Temperatures at 850 hPa rose gradually for the next 48 h (Figs. 8b and 8c), but with an episode of stronger warm air advection occurring as the winds strengthened on the afternoon of 4 January (Fig. 8c) and persisted on 5 January (Fig. 8d), bringing the 850-hPa temperature to about 6°C . The warm advection gave way to cold advection on the afternoon of 6 January as a short-wave trough was carried through the mean ridge position, dropping temperatures to around 0°C (Figs. 8e and 8f).

Meteorological observations within the Pasco basin (Fig. 9) agree well with the preceding synoptic description. The cold pool began in the early evening of 2 January as temperatures dropped in the basin (Fig. 9a) during a period of clear skies. The nighttime cooling produced persistent fog on the morning of 3 January. The fog cleared briefly at 0400 LST on 4 January, exposing an altocumulus overcast. By the next hour the fog had returned and lifted to form stratus. The fog and stratus persisted in the basin, decreasing the radiation input into the basin during the next two days (Fig. 9b) and suppressing the nighttime cooling (Fig. 9a). Long-wave radiation loss and cooling at the top of the fog deck destabilized the cloudy layer in the lowest 150–350 m of the basin atmosphere. The stability in this layer became nearly moist adiabatic and observations over the next two days in the basin included stratus, fog, mist, and freezing fog. A period of strong warm

air advection above the basin began in the late morning of 4 January. This advection produced a sharp temperature inversion at the top of the cold pool. The strong stability of this elevated layer decreased in intensity after noon on 6 January as cold air advection began above the pool. At 0400 LST on 6 January the fog deck cleared and an overcast of altocumulus and cirrus was observed until 2100 LST. The decreasing low cloudiness allowed sunlight to penetrate into the basin, producing convective warming at the base of the cold pool in the afternoon of 6 January, nearly destroying it. The cold pool restrengthened, however, following sunset and was finally destroyed the next day by convective warming at its base when the low clouds dissipated and overcast-to-broken altocumulus and cirrus were observed above the basin.

Winds were light (Fig. 9d) and variable (Fig. 9c) within the cold pool during the entire period. At about 1000 LST on 4 January strong winds intruded into the upper and middle elevations of the basin. Following this initial intrusion, moderate winds above the basin maintained a mostly westerly direction. The west winds aloft ended rather abruptly about 0800 LST on 6 January. After noon on this day, moderate winds began again aloft, but from a northwesterly direction, and the winds in the lower altitudes of the basin became westerly or northwesterly. As was the case for the December cold pool, pressures (Fig. 9e) were generally decreasing, with high relative humidity within the pool (Fig. 9f). No precipitation occurred during the January episode.

The evolution of the temperature profiles is shown at selected intervals from 1200 LST 4 January to 1200 LST 7 January 1999 in Fig. 10 using data from the collocated RASS and 122-m tower, and from temperature pseudoprofiles obtained from the lines of temperature dataloggers on Rattlesnake and Gable Mountains. Surface winds on the summit of Rattlesnake Mountain are also shown in the figure. Note from section 3 that there are differences in averaging times between sensors as well as spatial differences between the profiles and pseudoprofiles. The temperatures in the cold pool reported by the different sensors are similar during the period shown and have the characteristic near-moist-adiabatic gradient in the cloud-capped, surface-based layer. Strong warm air advection first began at about 1200 LST on 4 January at the highest altitudes (Fig. 10a). Over the course of time, the warm air descended progressively to lower elevations (Figs. 10b,c). The contrast between the warm air aloft and the cold air within the cold pool produced a strong temperature jump at the top of the cold pool over a depth of several hundred meters. Turbulent erosion produced by shear may have played a role in the descent of this feature. By 1200 LST on 6 January (Fig. 10d) warming inside the cold pool and cooling near its top had reduced the strength of the capping inversion. After nightfall, a strong surface-based inversion re-formed (Fig. 10e). This was de-

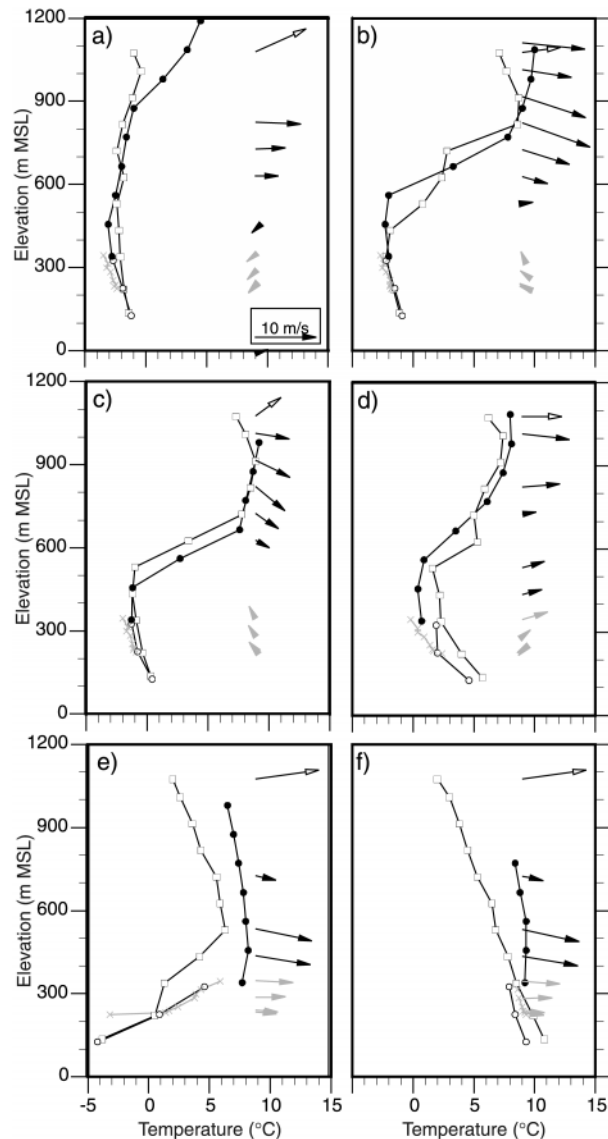


FIG. 10. Evolution of vertical temperature and wind structure as the Columbia basin cold pool forms and is destroyed during the period 4–7 January 1999. Shown are temperature and wind profiles at (a) 1200 LST 4 Jan, (b) 0000 LST 5 Jan, (c) 1200 LST 5 Jan, (d) 1200 LST 6 Jan, (e) 0000 LST 7 Jan, and (f) 1200 LST 7 Jan 1999. The symbols were defined in the caption of Fig. 7.

stroyed the next day (Fig. 10f) by a convective boundary layer that grew upward from the ground.

During the descent of the strong temperature jump at the top of the cold pool, large temperature oscillations occurred at the Hobo dataloggers on the mountainside as shown in Fig. 11. The oscillations appear to be produced by seiches or gravity waves that lap against the inclined terrain. The highest peak-to-peak oscillations (about 9°C) occur at altitudes corresponding to the layer of strong stability near the top of the cold pool where vertical temperature gradients are strongest. The amplitude of the oscillations is, no doubt, somewhat un-

derestimated by the long response time of these temperature sensors. The 5-min sampling rate does not allow us to resolve the periods of the oscillations. At lower altitudes within the cold pool, where the cloudy atmosphere is moist adiabatic, the temperature oscillations did not occur.

6. Discussion

The temperature deficit within the cold pool relative to the air above the pool (i.e., the cold pool *strength*) increases when the stability or cold pool depth increase, and decreases when the stability or depth decrease (Whiteman et al. 1999a). The many processes that can produce changes in atmospheric stability can be illustrated by an equation for local changes in lapse rate (Air Weather Service 1979):

$$\frac{\partial \gamma}{\partial t} = \underbrace{-\frac{1}{c_p} \frac{\partial}{\partial z} \left(\frac{dQ}{dt} \right)}_{\text{I}} - \underbrace{\mathbf{V}_H \cdot \nabla \gamma}_{\text{II}} + \underbrace{\frac{\partial \mathbf{V}_H}{\partial z} \cdot \nabla T}_{\text{III}} + \underbrace{\frac{\partial w}{\partial z} (\Gamma_d - \gamma)}_{\text{IV}} - \underbrace{w \frac{\partial \gamma}{\partial z}}_{\text{V}}, \quad (1)$$

where $\gamma = -\partial T/\partial z$ (lapse rate), t is time, c_p is the specific heat of air at constant pressure, z is height, Q is the heat supplied to a unit mass of air, \mathbf{V}_H is the horizontal wind vector, T is temperature, w is vertical wind, and Γ_d is the dry-adiabatic lapse rate. Equation (1) states that changes in stability can be caused by differential heating in the vertical (term I), advection of air of different stability (term II), differential temperature advection (term III), shrinking and stretching of the column (term IV), and vertical advection of lapse rate (term V). Stability increases when the lapse decreases with time (i.e., when $\partial \gamma/\partial t < 0$). The latent heat exchanged during condensation or evaporation, and heat transfers by radiation and turbulence are included in Q .

The cold pool formation and destruction mechanisms were different for the 24–26 December and 2–7 January cases. The December cold pool formed as static stability increased when relatively warm air was advected aloft over the basin (term III). Stratus suppressed the diurnal warming/cooling cycle in the pool (term I), and the pool was destroyed rather suddenly when cold air at the ground was replaced by warm air (terms II and V). The warm, unstable air was mixed down from aloft by flow over the topography at the southern end of the Pasco subbasin. The January cold pool began with a nocturnal inversion that formed in the basin on a clear night (term I). It was maintained by a stratus overcast that suppressed the diurnal warming in the basin (term I), was subsequently strengthened by warm air advection aloft (term III), was then weakened by cold air advection aloft

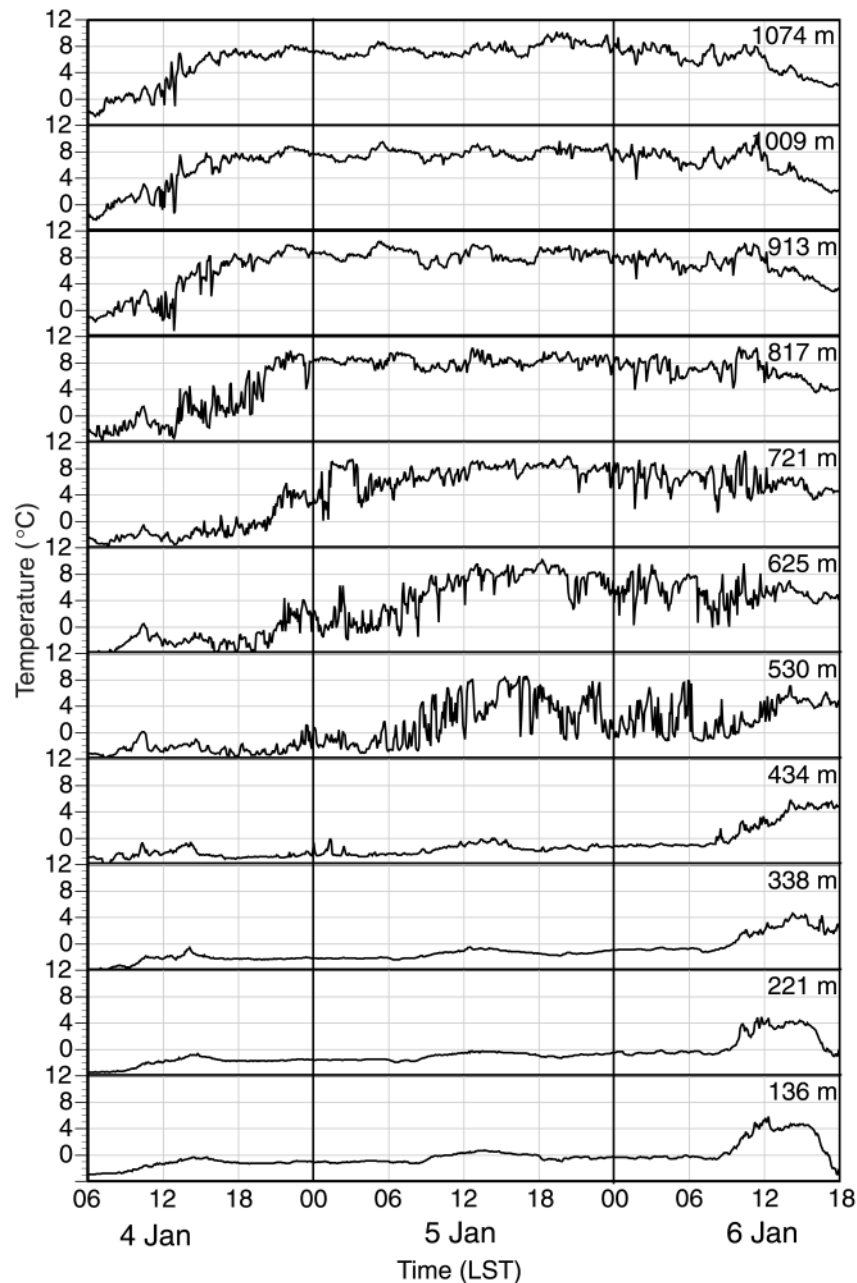
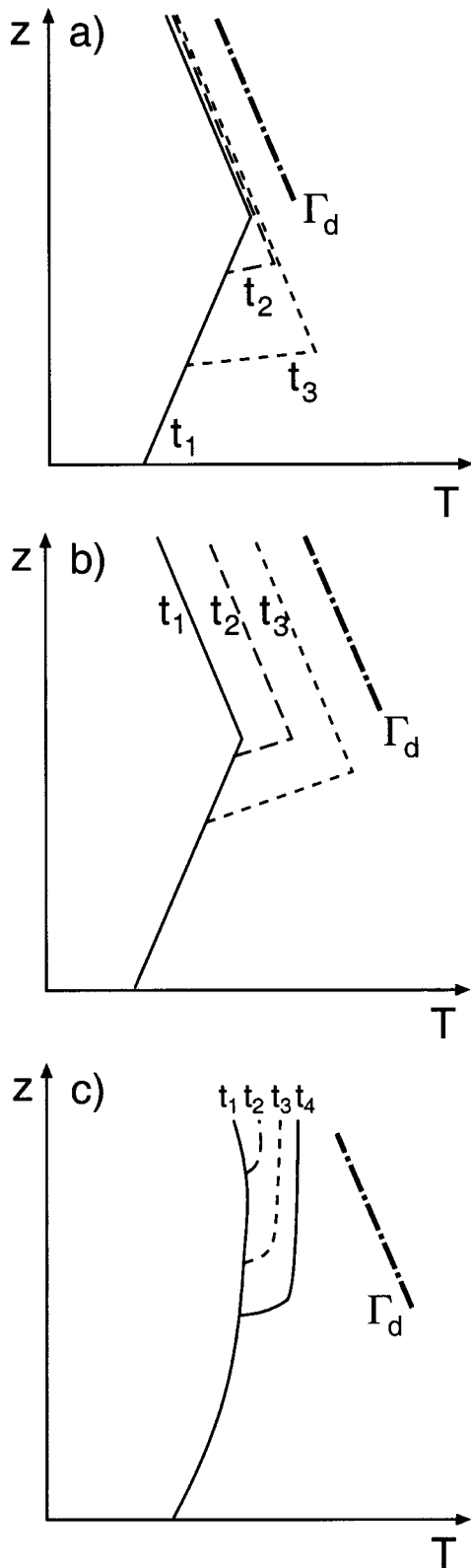


FIG. 11. Temperature time series at different heights on Rattlesnake Mountain from the 5-min Hobo data.

(term III), and was finally destroyed by convective boundary layer growth after the cloud cover dissipated (term I). While we have emphasized the major processes causing stability changes in the two episodes and their varying importance with time, it is clear that the terms in (1) are additive and that there are often cases where multiple processes are acting. A more complete treatment of the energetics of basins that may lead to further information on the roles of the various processes can be obtained by integrating over different layers the tem-

perature tendency equation from which (1) is derived. This has been done previously for Colorado's Sinbad basin (Whiteman et al. 1996; Fast et al. 1996) and for the Colorado Plateau basin (Whiteman et al. 1999a).

Because this paper describes the first observational investigation of cold pool structure in the Columbia basin, we would like to make further remarks on several cold pool topics. The topics include 1) horizontal homogeneity within the pool, 2) contributions of foehn or downslope winds to warming above the pool, 3) tur-



bulent erosion at the top of the pool, and 4) the role of clouds within the pool.

During the January episode when clouds were present within the cold pool, the RASS temperatures over the basin center differed little from the Hobo temperatures on nearby Rattlesnake Mountain (Fig. 10). This suggests that an assumption of horizontally homogeneity of temperatures within a cold pool may be valid in these circumstances. In strongly stable cold pools, buoyancy effects tend to keep isentropes and isotherms approximately horizontal even in cloudless conditions during daytime when one side of the basin is heated by the sun (Whiteman et al. 1999a). Strong temperature differences can occur, however, at the base of the cold pool between isolated subbasins (Whiteman et al. 1999a). The December cold pool exhibited strong horizontal temperature differences across the basin but these differences were not within the cold pool; rather, they were between cold pool remnants and the warmer air being mixed down from aloft that was replacing the cold air at the south end of the basin. The operation of the RASS and Hobo dataloggers during the whole winter of 1998/99 allows the possibility of investigating how stability within the basin affects the horizontal temperature differences between the basin center and Rattlesnake Mountain, the subject of a future article.

The strong warming above the basin on 4 January (Fig. 9) occurred with moderate west winds in a slightly stable air mass flowing over the Cascade Mountains. Some of this warming may have been caused by adiabatic descent of the flow on the lee side of the Cascades. Comparison of rawinsonde soundings upwind and downwind of the Cascades at Quillayute and Spokane, Washington, did not identify any temperature excesses on the east side of the Cascades. Because the adiabatic warming can occur locally over lee slopes and may not be apparent east of the mountains at Spokane, we investigated this further with a mesoscale numerical model and found a significant adiabatic warming component (Zhong et al. 2001).

Turbulent erosion has been proposed by previous investigators (e.g., Ayer 1961; Davidson and Rao 1963; Lenschow et al. 1979) as a potential mechanism for the descent of the top of a cold pool. Descent was a feature of the January episode, especially during the period from 1200 LST 4 January through 1500 LST 5 January (Fig. 10). Turbulent erosion is a process that removes the stable air layer by layer at the top of a cold pool by

←

FIG. 12. Schematic diagram of vertical soundings at successive times t_1 , t_2 , t_3 , etc., illustrating the evolution of temperature structure with (a) turbulent erosion (b) turbulent erosion with warm air advection aloft, and (c) differential warming aloft and then progresses downward with time. Panel (a) could also represent a combination of turbulent erosion and subsidence. The dry-adiabatic lapse rate ($\Gamma_d = -\partial T/\partial z = 9.8^\circ\text{C km}^{-1}$) is shown for comparison.

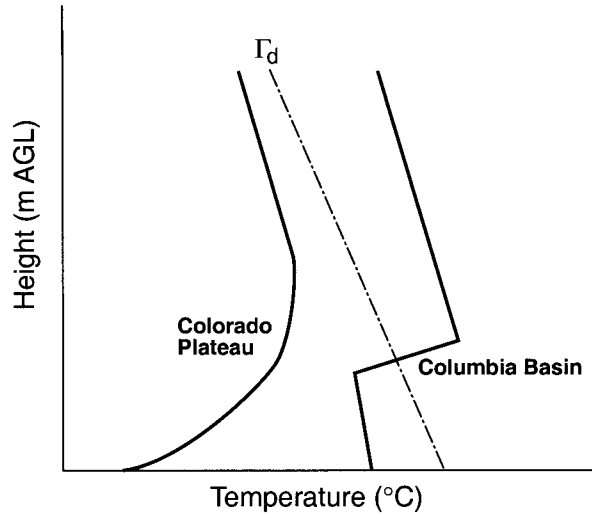


FIG. 13. Schematic of the different shapes of cold pool temperature profiles in the Colorado Plateau and Columbia basins. In noncloudy conditions in the Colorado Plateau (Whiteman et al. 1999a), stability decreases smoothly with height to the top of the cold pool. In contrast, cloudy cold pools in the Columbia basin have a near-moist-adiabatic, cloud-containing layer that is surmounted by a sharp temperature jump. The dry-adiabatic lapse rate (Γ_d) is shown for comparison.

turbulent eddies that are generated by wind shear between the quiescent air within the cold pool and stronger winds just above the stable transition layer at the top of the cold pool. Unfortunately, the radar profiler wind data were of insufficient quality to calculate Richardson numbers at the top of the cold pool to determine whether this mechanism is likely. Turbulent erosion can also occur with warm air advection above the cold pool. It is sometimes difficult to separate these turbulent erosion situations from differential advection in which warm air comes in first aloft, since all three situations can increase the temperature jump at the top of the cold pool and cause the cold pool top to descend (Fig. 12). Paradoxically, despite the fact that turbulent erosion and differential advection increase the strength of the temperature jump, turbulent erosion destroys the cold pool while warm air advection aloft strengthens it.

The role of turbulent erosion is also unclear for the December cold pool. The descent of the top of the cold pool over the south side of the Pasco subbasin was accomplished with a substantial static stability just above the interface (Fig. 10) and no wind speed observations were available above this interface. A second, related, hypothesis is that a hydraulic flow or descending air depressed the southern edge of the cold air mass and pushed it progressively northeastward. Turbulent erosion at the top of the depressed cold pool would increase the effectiveness of this mechanism. In future work we plan to investigate the turbulent erosion mechanism further using additional field data and numerical model simulations.

Fog and stratus were present in both Columbia basin cold pool episodes. Condensation within the pool may

be produced by cooling or moistening of the basin air. Evaporation may come from the basin floor or the Columbia River, which remains ice free in winter. The Pasco subbasin is a semiarid area receiving only about 0.16 m of precipitation annually. The soil moisture is relatively high in winter, however, as the basin receives its peak precipitation in this season. Fog and stratus in the January episode formed following nighttime cooling (Fig. 9) under clear skies. In contrast, stratus clouds in the December episode formed with little cooling during a light snowfall late on 23 December and in the morning of 24 December, and evaporation following these events probably played a role. When present, low clouds reduce diurnal temperature changes within the basin by reducing incoming solar radiation during daytime and reducing outgoing longwave radiation at night. Enhanced longwave radiative loss and cooling are produced at the cloud top during both day and night. The subsequent sinking of the cold air produces a distinctive near-moist-adiabatic lapse rate within the cloudy cold pool below. The formation of the fog and clouds releases latent heat within the Columbia basin cold pool; destruction of the pool requires that latent heat be supplied to evaporate this cloud water. The amount of latent heat can be significant. For example, a cloudy cold pool of 500-m depth with a constant potential temperature gradient of 14 K km^{-1} and a liquid water content of 0.5 g m^{-3} can be destroyed if all the air within the pool is brought to the same potential temperature as the cold pool top. Assuming a 1 m^2 column, the latent heat required to evaporate the cloud water would be 0.625 MJ and the sensible heat required to warm the dry air would be 1.75 MJ. Thus, latent heat would be 26% of the total heat required to destroy the cold pool.

The distinctive near-moist-adiabatic layer within the cold pool, when combined with the temperature jump at its top, distinguishes cold pool profiles in the Pasco basin from those observed previously in the center of the broad Colorado Plateau basin (Fig. 13) where low cloud cover is much less frequent and where the surrounding high plateaus have a continuous wintertime snow cover that increases longwave radiation loss and generates a flow of cold air into the basin, producing frequent surface-based temperature inversions. Temperature jumps similar to those seen in the Pasco basin have, however, been reported near the rim level of the Grand Canyon of the Colorado River (Whiteman et al. 1999b) where they are attributed to warm air advection above the canyon at times when colder air is confined in the narrow canyon below. During these events, similar temperature jumps are not seen over the broader Colorado basin, apparently because the warm air advected above the cold pool becomes better mixed with the air below during the long trajectory over the broad basin. Thus, the strength of a temperature jump above a basin may depend on distance from the surrounding or confining terrain.

7. Conclusions

We have defined a cold pool as a topographically confined, stagnant layer of air that is colder than the air above. Persistent multiday cold pools occur primarily in winter when the daily cycle of sensible heating and convection are insufficient, either because of cloudiness or seasonal reductions of sensible heat flux, to destroy the near-ground stable layer on a daily basis. Persistent cold pools in the Columbia basin often have a layer of enhanced stability at their top separating them from the warmer air above and, if stratiform clouds or fog form within the pool, the surface-based layer capped by the clouds is characterized by a near-moist-adiabatic lapse rate. Using our cold pool definition and considering a persistent cold pool to be one that lasts more than 18 h, we have developed a climatology of cold pools in the Columbia basin. On average, 11.6 cold pools occur per winter producing 399 cold pool hours per year.

An investigation of two persistent wintertime cold pools in the Columbia basin found different mechanisms for their initiation and decay. The first cold pool formed through a stabilization of the basin temperature profile as warm air was advected above the basin by synoptic-scale flows. The cold pool destruction was initiated when strong above-mountain winds shifted direction to bring stable air perpendicularly across the mountain crest at the south end of the Pasco subbasin, initiating a strong lee wave or hydraulic flow on the lee slopes of the Rattlesnake Ridge and Horse Heaven Hills. The cold pool was destroyed as the descending warm air progressively displaced more and more of the cold air in the basin. Remnants of the cold air remained trapped for some time in the lowest-lying terrain along the rivers. The second cold pool formed initially within the topography of the Pasco subbasin when fog and clouds developed within a nocturnal temperature inversion at the end of a clear night. Continued warm air advection aloft caused a sharp stable layer to form at the top of the pool. The synoptic-scale advection of warm air aloft may have been supplemented by mesoscale adiabatic warming by a chinook wind that descended from the Cascade Mountains to the west of the basin (Zhong et al. 2001). Fog that formed within the mesoscale pool lifted to form stratus. Cold air produced by radiative processes at the top of the stratus deck effectively stirred the pool through downward convection, producing a distinctive near-moist-adiabatic temperature structure within the pool. The stratus clouds kept direct sunlight from penetrating to the floor of the basin, effectively precluding the destruction of the cold pool by convective boundary layer growth. A layer of strong stability at the top of the cold pool, with relatively strong winds above, descended into the basin during the cold pool period. This descent occurred as the cold pool was strengthening (since the winds were bringing in warm air aloft). Insufficient data were available to test the hypothesis that turbulent erosion played a role in caus-

ing the strong stability cap at the top of the cold pool to descend. The cold pool was finally destroyed when cold air advection aloft destabilized the basin atmosphere, the stratus began to break, sunlight penetrated into the basin, and convection destroyed the cold pool from below.

Cold pool evolution is produced by atmospheric processes that occur on multiple scales (synoptic-scale differential temperature advection, subsidence, local evaporation and cooling, radiative processes at the cloud top, latent heat release caused by cloud microphysical processes, development of convection over the basin floor, downslope warming, etc.). The large number of processes and the multiplicity of scales present significant challenges for the numerical modeling and forecasting of cold pool buildup and breakdown. Forecasting the timing of the breakup of the cold pool is a particular challenge since there are instances when passing low pressure systems can leave the cold pool intact. Forecasts of precipitation type and timing, temperature maxima and minima, and the effects of these parameters on transportation and other activities depend critically on the cold pool forecast.

Vertical temperature and wind structure information is often unavailable in basins and valleys. The present study shows, however, that useful vertical temperature structure information may be obtained from inexpensive temperature dataloggers or weather stations on exposed mountainsides. To be of use in forecasts, this information would need to be available in real time.

While this paper has focused on two cold pool episodes in the Columbia basin it is not yet clear to what extent these episodes are representative of Columbia basin cold pools or of cold pools in different topographic settings. Because of the limited observational evidence and the variety of possible physical mechanisms that could result in the buildup and breakdown of the cold pools, further analysis and modeling will be required to gain a full understanding of wintertime cold pools. A related article by Zhong et al. (2001) extends the analysis of the January cold pool case with a mesoscale numerical model.

Acknowledgments. We thank the personnel at the Hanford Meteorological Station, especially Ken Burk, Gary Reinecke, Perry Perrault, and Dana Hoitink, for access to the weather station data and for discussions on cold pool forecasting and mechanisms. Bruce Bauck at the National Weather Service Forecast Office in Pendleton also provided helpful discussions. We thank two unidentified reviewers for their valuable comments. This research was supported by the U.S. Department of Energy, Office of Biological and Environmental Research, Environmental Sciences Division as part of their Environmental Meteorology Program under Contract DE-AC06-76RLO 1830 at PNNL. The U.S. Department of Energy's PNNL is operated by Battelle Memorial Institute.

REFERENCES

- Air Weather Service, 1979: The use of the skew T, log p diagram in analysis and forecasting. AWS/TR-79/006 Revised, 157 pp. [Available from U.S. Air Force Air Weather Service, Scott Air Force Base, IL, 62225-5008.]
- Ayer, H. S., 1961: On the dissipation of drainage wind systems in valleys in the morning hours. *J. Meteor.*, **18**, 560–563.
- Davidson, B., and P. K. Rao, 1963: Experimental studies of the valley–plain wind. *Int. J. Air Water Pollut.*, **7**, 907–923.
- Fast, J. D., S. Zhong, and C. D. Whiteman, 1996: Boundary layer evolution within a canyonland basin. Part II: Numerical simulations of nocturnal flows and heat budgets. *J. Appl. Meteor.*, **35**, 2162–2178.
- Furger, M., C. D. Whiteman, and J. M. Wilczak, 1995: Uncertainty of boundary layer heat budgets computed from wind profiler/RASS networks. *Mon. Wea. Rev.*, **123**, 790–799.
- Gill, G. C., 1983: Comparison testing of selected naturally ventilated solar radiation shields. NOAA Data Buoy Office Rep. (partial fulfillment of Contract NA-82-OA-A-266), 38 pp. [Available from NOAA/National Data Buoy Center, Bay St. Louis, MS 39529.]
- Lenschow, D. H., B. B. Stankov, and L. Mahrt, 1979: The rapid morning boundary-layer transition. *J. Atmos. Sci.*, **36**, 2108–2124.
- Mayr, G. J., and T. B. McKee, 1995: Observations of the evolution of orogenic blocking. *Mon. Wea. Rev.*, **123**, 1447–1464.
- Petkovšek, Z., 1974: Dissipation of the upper layer of all-day radiation fog in basins. *Zb. Meteor. Hidrol. Rad.*, **5**, 71–74.
- , 1978: Model for the evaluation of mean emission potential of the air pollution with SO₂ in basins. *Arch. Meteor. Geophys. Bioclimatol.*, **26B**, 199–206.
- , 1980: Dynamik der oberen Grenze der Kaltluftseen in Talbecken. *Abhandlungen des Meteorologischen Dienstes der Deutschen Demokratischen Republik*, Vol. 16, No. 124, 63–65.
- , 1992: Turbulent dissipation of cold air lake in a basin. *Meteor. Atmos. Phys.*, **47**, 237–245.
- Sauberer, F., and I. Dirmhirn, 1954: Über die Entstehung der extremen Temperaturminima in der Doline Gstettner-Alm (On the occurrence of extreme temperature minimums in the Gstettner-Alm Doline). *Arch. Meteor. Geophys. Bioclimatol.*, **5B**, 307–326.
- Savoie, M. H., and T. B. McKee, 1995: The role of wintertime radiation in maintaining and destroying stable layers. *Theor. Appl. Climatol.*, **52**, 43–54.
- Smith, R. B., J. Paegle, T. Clark, W. Cotton, G. Forbes, J. McGinley, H.-L. Pan, and M. Ralph, 1997: Local and remote effects of mountains on weather: Research needs and opportunities. *Bull. Amer. Meteor. Soc.*, **78**, 877–892.
- Vrhovec, T., 1991: A cold air lake formation in a basin—A simulation with a mesoscale numerical model. *Meteor. Atmos. Phys.*, **46**, 91–99.
- , and A. Hrabar, 1996: Numerical simulations of dissipation of dry temperature inversions in basins. *Geofizika*, **13**, 81–96.
- Whiteman, C. D., 1990: Observations of thermally developed wind systems in mountainous terrain. *Atmospheric Processes over Complex Terrain*, *Meteor. Monogr.*, Amer. Meteor. Soc., No. 45, 5–42.
- , T. B. McKee, and J. C. Doran, 1996: Boundary layer evolution within a canyonland basin. Part I: Mass, heat, and moisture budgets from observations. *J. Appl. Meteor.*, **35**, 2145–2161.
- , X. Bian, and S. Zhong, 1999a: Wintertime evolution of the temperature inversion in the Colorado Plateau basin. *J. Appl. Meteor.*, **38**, 1103–1117.
- , S. Zhong, and X. Bian, 1999b: Wintertime boundary layer structure in the Grand Canyon. *J. Appl. Meteor.*, **38**, 1084–1102.
- , J. M. Hubbe, and W. J. Shaw, 2000: Evaluation of an inexpensive temperature datalogger for meteorological applications. *J. Atmos. Oceanic Technol.*, **17**, 77–81.
- Wolyn, P. G., and T. B. McKee, 1989: Deep stable layers in the intermountain western United States. *Mon. Wea. Rev.*, **117**, 461–472.
- Zhong, S., C. D. Whiteman, X. Bian, W. J. Shaw, and J. M. Hubbe, 2001: Meteorological processes affecting the evolution of a wintertime cold air pool in the Columbia basin. *Mon. Wea. Rev.*, in press.